

Electronic structure of Ni-Cu alloys studied by spectroscopic ellipsometry

Kwang Joo Kim and David W. Lynch

Department of Physics and Ames Laboratory, U.S. Department of Energy, Iowa State University, Ames, Iowa 50011

(Received 19 December 1988)

Ellipsometric measurements of the complex dielectric functions of Ni and Ni_{1-c}Cu_c alloys ($c=0.1, 0.3, 0.4$) have been carried out in the (1.2–5.5)-eV region. Two structures in the σ_1 spectrum of pure Ni at about 1.5 and 4.7 eV are attributable to direct interband transitions in the band structure of ferromagnetic Ni. As the Cu concentration increases, the 4.7-eV edge (from transitions between the s - d -hybridized bands well below E_F and the s - p -like bands above E_F , e.g., $X_1 \rightarrow X'_4$) shifts to higher energies, while the 1.5-eV edge (from transitions between a p -like band below E_F and a d band above E_F along the L - W direction, e.g., $L'_2 \rightarrow L_3$) remains at the same energy. A structure grows in the (2–3)-eV region as Cu is added, and it is interpreted to be due to the transitions between the localized Cu subbands. All these observations are in accord with the calculated (coherent-potential-approximation) electronic structure of Ni-Cu alloys.

INTRODUCTION

The understanding of the electronic structure of disordered alloys is not yet as advanced as that of ordered crystals. Because of the lack of translational symmetry, the eigenstates of disordered alloys cannot be characterized in terms of the energy-band picture associated with Bloch's theorem, and often the nature of the one-electron states is not known.

A great deal of work has been done on the study of electron states in disordered, substitutional, binary alloys, which possess a regular crystal lattice whose sites are occupied at random by two different types of atoms. As a prototype of the nearly ideal, disordered, substitutional, binary-alloy systems, the electronic structure and related optical and magnetic properties of Ni-Cu alloys have long been the subject of much theoretical and experimental interest.

Ni and Cu are next to one another in the Periodic Table with atomic configurations $3d^9 4s^1$ and $3d^{10} 4s^1$, respectively, having the same fcc crystal structure, and the lattice constants differ by only about 2.5%. The electronic band structures of pure Ni (Refs. 1–3) and pure Cu (Refs. 4–6) are well known. Comparison of the two band structures reveals that the s - p bands are very similar in both metals and that they differ substantially in the location of the d bands with respect to the Fermi level E_F . There is a similarity in the optical properties of the two metals above 4 eV but a big difference at lower energies.^{7–11}

In the metallic state, Ni is known to have incompletely filled $3d$ bands and the magnetic exchange splitting of the spin-up and spin-down bands gives rise to ferromagnetism below T_c ($=633$ K).¹² Ni-Cu alloys are known to be ferromagnetic below a critical Cu concentration. Experimentally, it has been observed that the magnetic moment of the alloy disappears in the vicinity of 53 at. % Cu concentration.^{13,14}

To explain the decrease and disappearance of fer-

romagnetism with increasing Cu content in the Ni-Cu alloy system, the rigid-band model¹⁵ was proposed. It assumes that the alloy possesses one common band structure (mostly that of the host) and the density of states does not change its form, but only shifts rigidly as another component is added. Physically, this means that the electrons in the valence band are equally distributed between Ni and Cu sites and only a small constant change in the periodic potential is introduced. The common density of states of the alloy is filled up to E_F , determined by the electron-to-atom ratio. Hence, in the case of Ni-Cu, the d holes of Ni can be completely filled when the Cu concentration reaches about 60 at. % and this leads to the disappearance of the ferromagnetism. The fact that the magnetization in the Ni-Cu system is found experimentally to vanish at about this concentration has been taken to support the rigid-band model. But much experimental evidence^{16–23} showed that the rigid-band model is quite inappropriate to explain the electronic structure of Ni-Cu alloys in spite of the fact that Ni and Cu have very similar band structures. The same basic idea as the rigid-band model is used in the virtual-crystal-approximation description²⁴ in which the random array of potentials, V_A and V_B , of a binary alloy is replaced with an ordered array of potentials, $V_{\text{alloy}} = (1-c)V_A + cV_B$, where c is the concentration of species B . In common with the rigid-band model, the virtual-crystal approximation predicts one common-delocalized-band structure which shifts smoothly upon alloying, but it allows for deformation of the band shapes when the atomic composition is changed. This model can be a good approximation in describing the shape of the s - p bands of the alloy well above E_F .²¹

A different theoretical approach, called the minimum-polarity model,^{12,25,26} was proposed for Ni-Cu alloys. It assumes that the electronic configuration of each component in its pure-metal state carries over into the alloy. This implies local charge neutrality at each site and can be understood in the one-electron-band picture as the

limit in which the localization of the crystal is strong while the rigid-band model represents the opposite limit. Hence, the band structures of both species coexist without mixing with each other due to heavy scattering at the potential barrier between the two species. However, this model may also represent an oversimplification.

For dilute alloys where the interaction between solute atoms is not significant, the virtual-bound-state model²⁷ was proposed to explain the change of the electronic structures and the related optical properties of the alloys. It assumes that highly localized (in space and in energy) impurity states around the solute atoms are broadened in energy through a resonant scattering interaction with the nearly-free-electron-like bands of the host which are extended enough to overlap with the localized states. This model has been successful in describing the Ni-impurity *d* states in Cu-rich alloys, because they occur well separated in energy from the high-density Cu *d* bands.^{17,28,29}

It is more realistic to include the mixing of the adjacent states of Ni and Cu because they are expected to interact with each other. The theoretical approaches to this problem have involved multiple-scattering theory using the single-site approximation, which amounts to replacing the disordered, substitutional alloy by an equivalent perfect crystal of effective atoms where the electrons travel without being scattered. Two representative methods are the coherent-potential approximation (CPA) (Refs. 30–37) and the average-*t*-matrix approximation (ATA),^{38,39} the latter having the advantage of being simpler to implement than the former.

For a disordered, substitutional alloy the crystal momentum **k** is not a good quantum number and no well-defined *E*-**k** relation exists. Hence, the Bloch spectral function *a*(**k**, *E*), which can be interpreted as the density of states per **k** point, is as close as we can get to describing the electronic structure of the alloy. For an ordered system $a(\mathbf{k}, E) = \sum_{\nu} \delta(E - E_{\nu, \mathbf{k}})$, where $E_{\nu, \mathbf{k}}$ is the energy of a Bloch state with band index ν and wave vector **k**. Thus, for a given **k**, *a*(**k**, *E*) consists of a set of δ -function peaks and the positions of these peaks as a function of **k** is the *E*-**k** curve in an ordered system. In the case of a random alloy, *a*(**k**, *E*) broadens but usually remains well defined, the peak position and the width representing the quasiparticle energy and inverse lifetime of the complex energy band, respectively. The integral of *a*(**k**, *E*) over the first Brillouin zone is the configurationally averaged density of states $N(E) = (1 - c)N^A(E) + cN^B(E)$, where $N^A(E)$ and $N^B(E)$ are the contributions to the $N(E)$ from *A* and *B* sites, respectively. Despite the mathematical complexity of these calculations, the resultant electronic structure and density of states do not suffer the restrictions of the previous simple models. A knowledge of the evolution of the electronic structure of Ni-Cu alloys obtained by these calculations is desirable for explaining the change of the magnetic properties as well as the optical properties of this alloy system.

In the following, we report measurements of the complex dielectric functions, $\tilde{\epsilon} = \epsilon_1 + i\epsilon_2$, of Ni-Cu alloys in the (1.2–5.5)-eV region. The observed spectral features will be interpreted in terms of direct interband transitions between electronic states in the one-electron-band struc-

ture. We use $\sigma_1 = \omega\epsilon_2/4\pi$, the optical conductivity, and $\Delta\sigma_1 = (\sigma_1)_{\text{alloy}} - (\sigma_1)_{\text{pure}}$ to help in analyzing the evolution of the optical properties of the alloys which are related to the changes of the electronic structure due to alloying.

EXPERIMENT

Single-crystal Ni of (110) orientation and single crystals of Ni_{1-c}Cu_c (*c* = 0.1, 0.3, 0.4) of (100), (100), and (110) orientations, respectively, were cut and mechanically polished to a mirror finish with abrasives, the final grade being a paste of 0.05- μm -diam alumina.

The scanning photometric ellipsometer system with rotating polarizer and analyzer, both rotating synchronously at rotation rates of $\Omega/2$ and Ω ($f = 51$ Hz), which has been discussed in detail in Ref. 40, was used in this measurement.

Through the measurement of the amplitudes of the three ac components at frequencies of 51, 102, and 153 Hz, the complex-reflectance ratio, $\tilde{\rho} = \tilde{r}_p/\tilde{r}_s$, of the *p* (parallel) and *s* (perpendicular) field components of the light beam defined with respect to the plane of incidence of the sample is calculated. The complex dielectric function $\tilde{\epsilon}$ is related to $\tilde{\rho}$ through the equation

$$\tilde{\epsilon} = \sin^2\phi + \sin^2\phi \tan^2\phi [(1 - \tilde{\rho})/(1 + \tilde{\rho})]^2, \quad (1)$$

where ϕ is the angle of incidence of the light beam (68° in this measurement).

The complex dielectric functions of the samples have been determined in the (1.2–5.5)-eV photon-energy region at intervals of 0.01 eV in the (1.2–2.5)-eV range and 0.02 eV in the (2.5–5.5)-eV range. Measurement errors do not exceed 1% in ϵ_2 . Systematic errors due to the effect of oxide overlayer formation appear to be small, and partially cancel in the $\Delta\sigma_1$ spectra. They do not affect any conclusions drawn.

RESULTS

The real parts of the measured complex optical conductivities σ_1 of pure Ni and the three Ni-Cu alloys are displayed in Fig. 1. The spectrum for pure Ni shows two representative structures, a peak near 1.5 eV and a broad structure around 4.7 eV. As Cu is added, the intensities of both structures decrease, while a broad structure grows in the (2–3)-eV region. The peak position of the 4.7-eV structure shifts to higher energies as the Cu concentration increases, while that of the 1.5-eV structure remains unchanged, as listed in Table I.

In Fig. 2, $\Delta\sigma_1 = (\sigma_1)_{\text{alloy}} - (\sigma_1)_{\text{pure}}$ spectra are shown to demonstrate the evolution of the above-mentioned structures more clearly. The intensities of the two structures diminish gradually from those of pure Ni as the Cu concentration increases. We can also see that a broad structure in the (2–3)-eV region develops and its peak position shifts to lower energies as the Cu concentration increases. This shift is nearly linear with Cu concentration from 3.0 eV for 10 at. % Cu to 2.7 eV for 40 at. % Cu. The intensity of this structure increases nearly linearly in the Cu

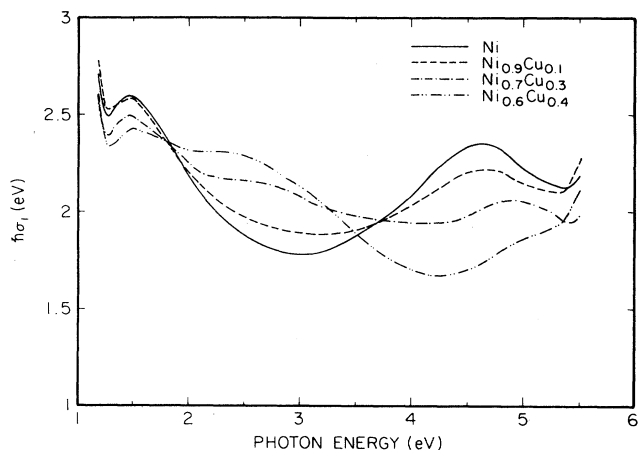


FIG. 1. Real part of the complex optical conductivity σ_1 vs photon energy for $\text{Ni}_{1-c}\text{Cu}_c$.

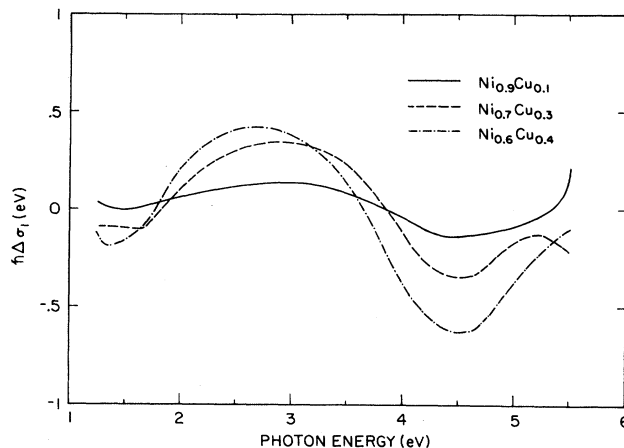


FIG. 2. The change in the real part of the complex optical conductivity $\Delta\sigma_1$ vs photon energy for $\text{Ni}_{1-c}\text{Cu}_c$.

concentration as shown in Fig. 3. The reflectivity spectra, defined by

$$R = [(n-1)^2 + k^2] / [(n+1)^2 + k^2], \quad (2)$$

with $\epsilon_1 = n^2 - k^2$ and $\epsilon_2 = 2nk$, agree very well with the spectra reported by Feinleib *et al.*⁴¹ The shift of the minimum point of the spectra is listed in Table I.

DISCUSSION

A number of measurements of the dielectric functions of Ni have been reported, but substantial disagreement is found in the shape of the spectrum⁴²⁻⁴⁴ and in the assignments of the optical structures^{7,8,44-48} found in the spectrum.

The optical structure at about 1.5 eV has been assigned to direct interband transitions between a p -like band below E_F and a d band above E_F along the $L-W$ direction,^{3,8,44,47} e.g., $L_2 \rightarrow L_3$, as indicated in the ferromagnetic band structure for Ni (Ref. 3) (Fig. 4), which has been obtained empirically by fitting angle-resolved photoemission results.^{49,50} The structure at about 4.7 eV has

TABLE I. Experimentally determined maximum positions in the optical conductivity σ_1 and minimum positions in the reflectivity R for $\text{Ni}_{1-c}\text{Cu}_c$.

| C | First maximum | Second maximum | Minimum R (eV) |
|-----|-----------------|-------------------|----------------|
| | σ_1 (eV) | σ_1 (eV) | |
| 0.0 | 1.47 | 4.65 | 4.07 |
| 0.1 | 1.47 | 4.67 | 4.27 |
| 0.3 | 1.47 | 4.89 | 4.69 |
| 0.4 | 1.49 | 4.97 ^a | 4.71 |

^aPhoton energy of minimum $d\sigma_1/d\omega$.

been assigned to direct interband transitions between the spatially extended $s-d$ -hybridized states well below E_F and the $s-p$ -like conduction states above E_F ,^{3,48} e.g., $X_1 \rightarrow X'_4$, as indicated in Fig. 4. The oscillator strength for these transitions is expected to be very sensitive to changes in the crystal potential because it is a sum of two interfering terms. It decreases significantly from Ni to Cu.⁴⁸

As the Cu concentration increases a structureless, broad "peak" appears in the (2-3)-eV region in the σ_1 spectra. It grows at the expense of the Ni-derived structures around 1.5 and 4.7 eV. Its peak position in the $\Delta\sigma_1$ spectra shifts to lower energies with increasing Cu concentration. Cu is known to have a main absorption edge at about 2.1 eV due to $L_3 \rightarrow L'_2$ (E_F) transitions,^{7,10,11,51} indicating that the position of the L_3 band is about 2.1

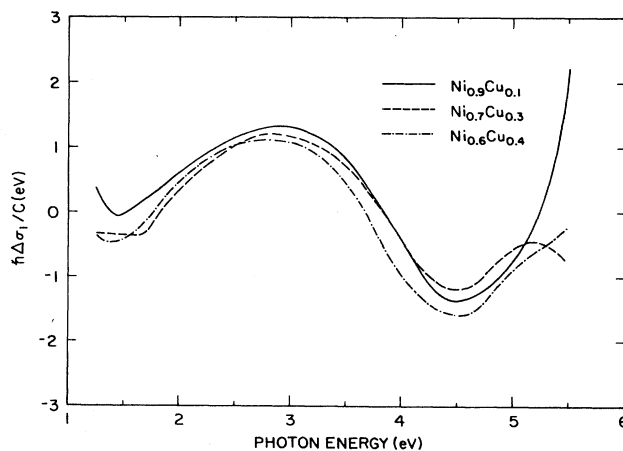


FIG. 3. The change in the real part of the complex optical conductivity divided by the Cu concentration $\Delta\sigma_1/c$ vs photon energy for $\text{Ni}_{1-c}\text{Cu}_c$.

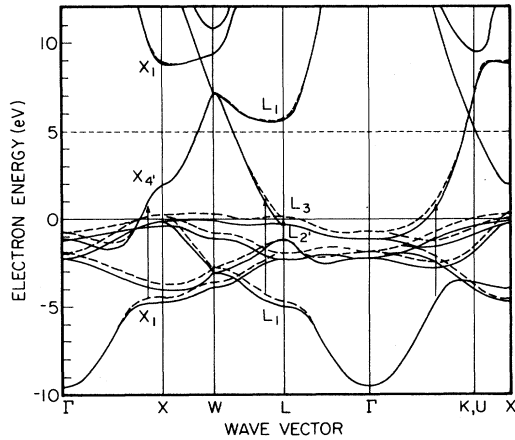


FIG. 4. Combined-interpolation-scheme band structure for ferromagnetic Ni (Ref. 3).

eV below E_F in pure Cu. Hence, the shoulder in the (2–3)-eV region is attributable to transitions involving the d states of Cu, which occur at lower energies than those of Ni.³⁹ The shift of the peak position in the $\Delta\sigma_1$ spectra is an indication of the upward shift of the L_3 band of Cu, which is attributable to the increase of the d -band width of Cu due to the increase of d - d overlap interactions among Cu atoms as the Cu concentration increases.

Therefore, it is expected that the d states of Cu and Ni are formed separately, even at low Cu concentrations. According to the CPA calculation by Munoz *et al.*,²¹ the partial densities of d -like states, $N^{\text{Ni}}(E)$ and $N^{\text{Cu}}(E)$, are quite different below E_F , which indicates that the wave functions tend to localize either on the Ni sites or on the Cu sites. Thus, below E_F the electronic structure of the Ni-Cu system is in the split-band behavior in which there are nearly separate Ni and Cu states. This behavior persists even above E_F (~ 1 eV) in their result, but reduces rapidly to $N^{\text{Ni}}(E) \sim N^{\text{Cu}}(E)$ at higher energies, to make the amplitude of the wave function comparable on both sites. Thus, a common band structure accommodates the electrons from both Ni and Cu well above E_F . In the band structure of pure Ni,³ the L'_2 band is completely filled and is located below the L_3 band while the L'_2 band is not completely filled and is located above the L_3 band in pure Cu. This is due to a big difference in the crystal potential between Ni and Cu that helps maintain the split-band behavior in the Ni-Cu alloy. Thus, the p -like L'_2 band of Cu is expected not to be shared by the electrons from Ni so that the intensity of the $L_3 \rightarrow L'_2$ (E_F) transitions is directly proportional to the concentration of Cu. The existence of a large density of Cu d states around 2–3 eV below E_F in Ni-Cu alloys has been confirmed in several photoemission measurements.^{17,19,22,23}

According to the CPA calculations for paramagnetic Ni-Cu alloys by Stocks *et al.*,^{30,33,36} the density of Cu d states is broad, with its center at about 3.5 eV below E_F

and a half-width of about 2 eV for 11 at. % Cu, as shown in Fig. 5. As the Cu concentration increases, these Cu $3d$ subbands grow to size comparable to that of the Ni d bands and become wider due to the increased overlap interaction among d electrons of Cu.

As the Cu-derived structure grows, the strength of the 4.7-eV structure in the σ_1 spectra, which is due to the transitions between lower s - d -hybridized states and s - p -like states above E_F , is reduced and its maximum position shifts to higher energies. The gradual decrease in the intensity of the structure is attributable to the decrease of the density of states of the Ni subbands as Ni atoms are replaced by Cu atoms. However, the s - d hybridization is not expected to decrease because both of the d bands are expected to hybridize with the conduction band, and the separation between the d states at about L_1 and the bottom of the conduction band, Γ_1 , in Cu, to which the hybridization is inversely proportional,⁴⁸ is close to that in Ni, from 4.5 eV in Ni to 3 eV in Cu.³⁹

It is reasonable to assume that the alloy has common s bands because the conduction electrons are expected to be highly delocalized. In this case it seems reasonable to treat the position of the bottom of the s band, Γ_1 , in the virtual-crystal approximation in which

$$\Gamma_1 = (1-c)\Gamma_1^{\text{Ni}} + c\Gamma_1^{\text{Cu}}. \quad (3)$$

Similarly, we suppose that the positions of the s - d -hybridized bands in the alloy takes the average of the positions of those in pure Ni and pure Cu,

$$E_{sd} = (1-c)E_{sd}^{\text{Ni}} + cE_{sd}^{\text{Cu}}. \quad (4)$$

According to the calculated band structure,³⁹ the posi-

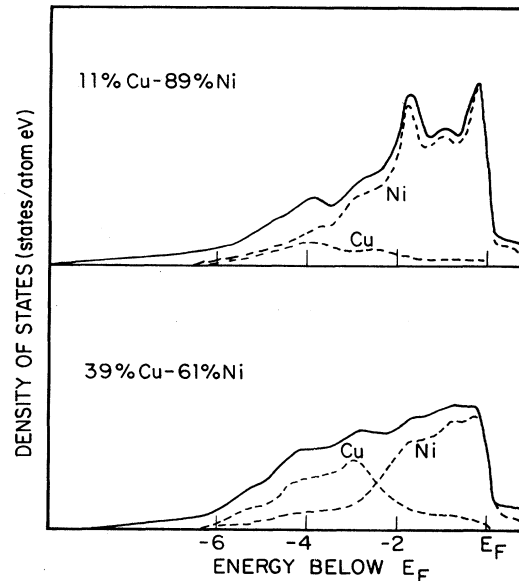


FIG. 5. Density of states for 11-at. %-Cu and 39-at. %-Cu alloys calculated using the CPA (Ref. 30). (Energies in eV.)

tions of X_1 and L_1 of pure Cu are lower by about 1 eV than those of pure Ni. Hence, as the Cu concentration increases, the nearly delocalized $s-d$ states around X_1 and L_1 are expected to shift down, making the edge of the 4.7-eV transitions shift to higher energies. By applying Eq. (4) we have the magnitudes of the shifts of the $s-d$ -hybridized states which agree with the shifts of the experimental spectra as listed in Table II.

The evolution of the 1.5-eV structure in the σ_1 spectra is expected to be related to the change of the ferromagnetism in Ni-Cu alloys because the transitions causing the structure involve the minority-spin d bands of Ni along the $L-W$ direction.

As was seen earlier, upon alloying, the d bands of Cu in Ni-Cu alloys are at lower energies than those of pure Cu, so that the alloy's Cu $s-p$ bands occur at lower energies than in pure Cu. Hence, the Fermi level of the Ni-Cu alloy may not shift upward with respect to the bottom of the conduction band, even though Cu has one more valence electron than Ni, and this does not agree with the rigid-band model.

According to the CPA calculation of Gordon *et al.* for a paramagnetic Ni-Cu alloy,³⁷ the Fermi level shifts down in the Ni-rich region as the Cu concentration increases, shifting by 0.3 eV at 39 at. % Cu. However, they interpreted this result as a failure in their description of the crystal potential. The Fermi energies of pure Ni and Cu are very close to each other, E_F of Ni being higher by only 0.08 eV than that of Cu, calculated from the bottom of each conduction band, and Γ_1^{Ni} is located higher by only 0.18 eV than Γ_1^{Cu} relative to the muffin-tin zero.³⁹

The density of states of pure Ni obtained from the calculated band structure² shows a sharp change of the density of minority-spin d states at E_F . Hence, if the Fermi level shifts relative to the location of the minority-spin d bands of Ni upon alloying, then the intensity of the 1.5-eV structure is expected to change rapidly as the Cu concentration changes. Our experimental result does not show a rapid decrease in the intensity of the 1.5-eV structure as the Cu concentration increases. Instead, it shows a rather gradual linear decrease in intensity, and this is more attributable to the decrease of Ni d states as Ni atoms are replaced by Cu atoms than to the relative shift of E_F from the d bands of Ni.

The CPA calculation of Inoue and Shimizu¹³ for a ferromagnetic Ni-Cu alloy on the assumption of the Hubbard model results in a gradual decrease in the ferromagnetism due to a relative shift of the majority-spin band of Ni relative to the minority-spin band to make the net magnetic moment of Ni approach zero. In other words, the magnetic exchange splitting between the majority- and minority-spin Ni-derived bands decreases as the Cu concentration increases. This behavior was predicted for Ni-Cu (Ref. 52) and the temperature depen-

TABLE II. Comparison of the shift of the minimum position of the reflectivity spectra with the calculated shift of the L_1 point based on Eq. (4) for $\text{Ni}_{1-c}\text{Cu}_c$. (The positions of L_1 for pure Ni and Cu are from Ref. 39.)

| C | Shift of minimum R (eV) | Shift of L_1 (eV) |
|-----|-------------------------------|------------------------|
| 0.1 | 0.20 | 0.17 |
| 0.3 | 0.62 | 0.50 |
| 0.4 | 0.64 | 0.67 |

dence of the energy gap for pure Ni was observed by polarization-dependent photoemission.⁴⁹ In this process, some of the d electrons from the majority-spin band of Ni transfer to the s band, leaving majority d holes which reduce the net magnetic moment of the alloy. The densities of states of the alloy obtained from this calculation are found to be strongly smoothed out by lifetime effects caused by a rather large difference in the crystal potential between Ni and Cu sites. In this case it is expected that there is negligible charge transfer from Cu sites to Ni sites due to strong scattering at the potential barrier between the two sites.

Therefore, the above result strongly suggests that the d holes at Ni sites are not filled by d electrons transferred from Cu sites, even at large Cu concentration, and this is close to the result from the minimum-polarity model proposed by Lang and Ehrenreich.^{12,25} According to this model, which assumes a random scattering potential strong enough to produce nearly independent Ni and Cu subbands, the d electrons of Cu are confined to the Cu sites, so that the Cu d bands are completely filled and reside below E_F . Then the d electrons near E_F come from only Ni sites. This charge neutrality of the Ni-Cu system was also indicated by the soft-x-ray-emission²⁰ and -absorption measurements.^{21,53}

Therefore, as the Ni concentration decreases, the density of states of the minority d bands decreases in proportion to that of the majority d bands and it leads to reducing the difference between the number of d -electrons with majority spin and that with minority spin so the ferromagnetism becomes reduced.

ACKNOWLEDGMENTS

The authors acknowledge useful conversations with Dr. B. N. Harmon. The Ames Laboratory is operated for the U. S. Department of Energy by Iowa State University under Contract No. W-7405-Eng-82. This work was supported by the Director for Energy Research, Office of Basic Energy Science.

¹E. I. Zornberg, Phys. Rev. B **1**, 244 (1970).

²J. Callaway and C. S. Wang, Phys. Rev. B **7**, 1096 (1973); **9**, 4897 (1974); **15**, 298 (1977).

³N. V. Smith, R. Lässer, and S. Chiang, Phys. Rev. B **25**, 793

(1982).

⁴G. A. Burdick, Phys. Rev. **129**, 138 (1963).

⁵R. Lässer, N. V. Smith, and R. L. Benbow, Phys. Rev. B **24**, 1895 (1981).

- ⁶H. Eckardt, L. Fritsche, and J. Noffke, *J. Phys. F* **14**, 97 (1984).
- ⁷H. Ehrenreich, H. R. Philipp, and D. J. Olechna, *Phys. Rev.* **131**, 2469 (1963).
- ⁸M. Shiga and G. P. Pells, *J. Phys. C* **2**, 1847 (1969).
- ⁹G. P. Pells and M. Shiga, *J. Phys. C* **2**, 1835 (1969).
- ¹⁰P. B. Johnson and R. W. Christy, *Phys. Rev. B* **6**, 4370 (1972).
- ¹¹P. B. Johnson and R. W. Christy, *Phys. Rev. B* **11**, 1315 (1975).
- ¹²N. D. Lang and H. Ehrenreich, *Phys. Rev.* **168**, 605 (1968).
- ¹³J. Inoue and M. Shimizu, *J. Phys. Soc. Jpn.* **4**, 1321 (1976).
- ¹⁴J. C. Ododo and B. R. Coles, *J. Phys. F* **7**, 2393 (1977).
- ¹⁵N. F. Mott, *Proc. Phys. Soc. London* **47**, 571 (1935); *Philos. Mag.* **22**, 287 (1936).
- ¹⁶L. E. Wallden, D. H. Seib, and W. E. Spicer, *J. Appl. Phys.* **40**, 1281 (1969).
- ¹⁷D. H. Seib and W. E. Spicer, *Phys. Rev. B* **2**, 1676 (1970); **2**, 1694 (1970).
- ¹⁸M. Tokumoto, H. D. Drew, and A. Bagchi, *Phys. Rev. B* **16**, 3497 (1977).
- ¹⁹B. Cordts, D. M. Pease, and L. V. Azaroff, *Phys. Rev. B* **22**, 4692 (1980).
- ²⁰P. J. Durham, D. Ghaleb, B. L. Györfy, C. F. Hague, J.-M. Mariot, G. M. Stocks, and W. M. Temmerman, *J. Phys. F* **9**, 1719 (1979).
- ²¹M. C. Muñoz, P. J. Durham, and B. L. Györfy, *J. Phys. F* **12**, 1497 (1982).
- ²²K. Y. Yu, C. R. Helms, W. E. Spicer, and P. W. Chye, *Phys. Rev. B* **15**, 1629 (1977).
- ²³P. Heimann, H. Neddermeyer, and M. Pessa, *Phys. Rev. B* **17**, 427 (1978).
- ²⁴L. Nordheim, *Ann. Phys. (Leipzig)* **9**, 607 (1931); **9**, 641 (1931).
- ²⁵S. Kirkpatrick, B. Velicky, N. D. Lang, and H. Ehrenreich, *J. Appl. Phys.* **40**, 1283 (1969).
- ²⁶S. Kirkpatrick, B. Velicky, and H. Ehrenreich, *Phys. Rev. B* **1**, 3250 (1970).
- ²⁷J. Friedel, *Nuovo Cimento Suppl.* **2**, 287 (1958); P. W. Anderson, *Phys. Rev.* **124**, 41 (1961).
- ²⁸C. L. Foiles, *Phys. Rev.* **169**, 471 (1968).
- ²⁹D. Beaglehole, *Phys. Rev. B* **14**, 341 (1976).
- ³⁰G. M. Stocks, R. W. Williams, and J. S. Faulkner, *Phys. Rev. B* **4**, 4390 (1971).
- ³¹V. Srivastava and S. K. Joshi, *Phys. Rev. B* **12**, 2871 (1975).
- ³²D. K. Ghosh and P. Bhattacharyya, *Phys. Rev. B* **11**, 2642 (1975).
- ³³G. M. Stocks, W. M. Temmerman, and B. L. Györfy, *Phys. Rev. Lett.* **41**, 339 (1978); *J. Phys. F* **8**, 2461 (1978).
- ³⁴A. Bansil, *Phys. Rev. Lett.* **41**, 1670 (1978).
- ³⁵A. Bansil, *Phys. Rev. B* **20**, 4025 (1979).
- ³⁶J. S. Faulkner and G. M. Stocks, *Phys. Rev. B* **21**, 3222 (1980).
- ³⁷B. E. A. Gordon, W. E. Temmerman, and B. L. Györfy, *J. Phys. F* **11**, 821 (1982).
- ³⁸A. Bansil, H. Ehrenreich, L. Schwartz, and R. E. Watson, *Phys. Rev. B* **9**, 445 (1974).
- ³⁹A. Bansil, L. Schwartz, and H. Ehrenreich, *Phys. Rev. B* **12**, 2893 (1975).
- ⁴⁰L.-Y. Chen and D. W. Lynch, *Appl. Opt.* **26**, 5221 (1987).
- ⁴¹J. Feinleib, W. J. Scouler, and J. Hanus, *J. Appl. Phys.* **40**, 1400 (1969).
- ⁴²A. A. Studna, *Solid State Commun.* **16**, 1063 (1975).
- ⁴³M.-Ph. Stoll, *J. Appl. Phys.* **42**, 1717 (1971).
- ⁴⁴D. W. Lynch, R. Rosei, and J. H. Weaver, *Solid State Commun.* **9**, 2195 (1971).
- ⁴⁵G. S. Krinchik and V. S. Gushchin, *Zh. Eksp. Teor. Fiz.* **56**, 1833 (1969) [*Sov. Phys.—JETP* **29**, 984 (1969)].
- ⁴⁶J. Hanus, J. Feinleib, and W. J. Scouler, *Phys. Rev. Lett.* **19**, 16 (1967).
- ⁴⁷J. Hanus, J. Feinleib, and W. J. Scouler, *J. Appl. Phys.* **39**, 1272 (1968).
- ⁴⁸F. M. Mueller and J. C. Phillips, *Phys. Rev.* **157**, 600 (1967).
- ⁴⁹F. J. Himpsel, J. A. Knapp, and D. E. Eastman, *Phys. Rev. B* **19**, 2919 (1979).
- ⁵⁰W. Eberhardt and E. W. Plummer, *Phys. Rev. B* **21**, 3245 (1980).
- ⁵¹E. Colavita, S. Modesti, and R. Rosei, *Solid State Commun.* **17**, 931 (1975).
- ⁵²E. P. Wohlfarth, *Rev. Mod. Phys.* **25**, 211 (1953).
- ⁵³W. Gudat and C. Kunz, *Phys. Status Solidi* **52**, 433 (1972).